Trace ammonium removal by liquid-liquid membrane contactors as water polishing step of water electrolysis for hydrogen production from wastewater treatment plant effluent

Edxon Eduardo Licon Bernal[1], Aurora Alcaraz[1], Sandra Casas[2], César Valderrama[1,*], José Luis Cortina[1,2]

[1] Departament d'Enginyeria Química, Universitat Politècnica de Catalunya, Spain.

[2] Water Technology Center CETaqua, Barcelona, Spain.

[*]Correspondence should be addressed to: César Valderrama

Departament d'Enginyeria Química, Universitat Politècnica de Catalunya.

Av. Diagonal 647 08028, Barcelona Spain.

Tel.: (+34) 93 4016997

Email: cesar.alberto.valderrama@upc.edu

Abstract

BACKGROUND: This work evaluates Hollow Fiber liquid-liquid Membrane Contactors (HFMC) as polishing step for the removal of low levels of ammonium from water purified by (or being supplied to) a membrane distillation unit in order to fulfil the conductivity requirements of the hydrogen production by water electrolysis.

RESULTS: The influence of the operational conditions (flow, pH, ammonium concentration, buffer capacity) were evaluated under a closed-loop setup in order to achieve a reduction of total ammonia concentration in water, from 15 up to 1 mg/L to assure the production of water in the membrane distillation with a conductivity lower than 1 µS/cm. These values were used to validate a numerical algorithm describing the system performance. In order to reach the ammonia concentration requirements and considering the low concentration of bicarbonate (low pH buffer capacity) on the treated water a buffer agent was added to the working solution.

CONCLUSIONS: HFMC technology is a suitable solution to remove low levels of ammonium from water to values up to 1 mg/LNH_3 through appropriate control of pH. The ammonium removal efficiency by HFMC was improved by raising the pH or the flow rate. Finally, the model proposed provides a good description of the membrane contactor performance with minimal deviations when compared with experimental results.

Keywords: ammonium removal; membrane contactor; hollow fiber; buffer solution; hydrogen production.

1. Introduction

The USA and European Roadmaps plans on energy efficiency established the need of evolution of the world fuel-based economy into a low carbon economy by 2050, which would lead to a reduction of the greenhouse gases emissions by 60-80%.[1] Recently, the European Union Life Project Greenlysis propose that wastewater treatment plants (WWTP) must not be seen just as industrial installations with certain potential to increase its energy efficiency, but also as producers of renewable energy and distribution networks of hydrogen for the transport sector.[1] Within this European context, WWTPs become an excellent location for hydrogen production through water electrolysis, which could be powered with renewable energies due to space availability in WWTPs for its installation. In addition, WWTPs have an excellent strategic geographical distribution to become effective hydrogen suppliers and oxygen obtained through water electrolysis can also be used in the WWTP itself.

A scheme based on the combination of membrane ultra-filtration and membrane distillation was proposed and evaluated for the removal of residual suspended solids, dissolved organic matter and dissolved ionic species. Membrane distillation (MD) is a membrane-based water treatment process where the driving force is a vapour pressure across the membrane, aiming to obtain

water with conductivity lower than 1 μS/cm in order to fulfil the quality requirements to feed the electrolyser (accepted < 5 μS/cm).

Nevertheless, the presence of low levels of ammonium, which can be transported through the hydrophobic pores of the membranes as $NH_{3(g)}$ decreases the quality of the evaporated water.[2] Such phenomenon increased the water conductivity to values higher than 1 μS/cm, reducing the production of hydrogen when the same amount of energy to produce the water splitting was applied. According to that, a final polishing step for the removal of low levels of ammonium ions from the aqueous solutions is a research need.

After a critical review of the conventional separation processes for ammonium/ammonia removal from water and wastewater, air stripping, selective ion exchange and break-point chlorination, were discarded as they not provide the removal requirements or due to the lack of simplicity on process integration.[3,4] Contrary, hollow-fiber membrane contactors (HFMCs) have attracted large attentions as an effective separation process especially when applied to treat clean process streams (e.g. removal of $N_{2(g)}$ gases from water in beer production, or removal of CO_2(g) in water demineralization units). Hydrophobic hollow fiber membrane contactors are used to extract dissolved gases (e.g. oxygen, $CO_{2(g)}$) from aqueous solutions.[5] Since the membrane is hydrophobic, wetting of the membrane pore is neglected. Gases are transported from the aqueous phase (feed solution) to the membrane phase up to the stripping solution. Typically this receiving solution is a liquid phase where the transported gases are solubilized and transformed onto ionic species as could be bicarbonate or carbonate for the case of carbon dioxide.[6] A major part of the interest toward HFMCs is due to their capability in providing a dispersion free of contact between two phases.[7] In comparison to conventional scrubbers membrane contactors have a much larger specific surface area, thus space requirements and capital costs are reduced.[8]

Operational parameters such as feed flow-rate, temperature and pH must be optimized to efficiently remove the gas species from the feed solution, especially when the speciation of the compound to be removed is pH dependent, as is the case of bicarbonate and ammonium ions. Ammonium is deprotonated onto ammonia at pH values higher than the pKa_{298K}=9.3 (equation 1) and when the aqueous solution contacts the pores filled with air, it could be converted to ammonia gas as described by equation 2. Therefore it is expected that the transport efficiency increases with the increase of the pH to values close or above 9.3.[5]

$$NH_4^+ \leftrightarrow NH_3 + H^+ \qquad pKa_{(298K)}=-9.3 \qquad (1)$$

$$NH_3 \leftrightarrow NH_{3(g)} \qquad K_{H\,(298K)}\ ((Pa\ m^3/mol) = 1.6 \qquad (2)$$

When it is compared to conventional absorption or stripping processes, such as bubble columns and packed beds, the use of hydrophobic hollow-fiber membrane contactors provides a number of advantages. These include: a larger interfacial area per unit volume, which provides fast removal of the volatile contaminants; independent control of the liquid and striping solution flow rates without causing any flooding, loading or foaming; Furthermore, due to the tangential nature of the flow in the membrane contactors (MC), the gas stripping process does not require operation at a high-pressure drop when working in liquid-gas mode. This also contributes to lower capital cost and ease of operation.[6,7]

However, the mass transfer of some volatile compounds (VC), such as NH_3, is a complex process due to its conversion to ionic forms (NH_4^+).[7] The initial pH and the variations of pH values during the operation process affect the rate of mass transfer. As NH_3 is converted onto NH_4^+, the relative concentrations of both species will be defined by the pH values of the feed. Thus, the influence of feed pH should be considered and assessed in order to enhance the ammonium removal.

The removal mechanism of ammonium using hollow fiber membrane contactors (HFMC) have been subject of many studies.[11-17] The cited studies were devoted to enhance ammonium

extraction efficiency optimizing the operation conditions to achieve high recovery ratios. However not efforts were addressed to achieve low levels of ammonium concentration on the treated water. Additionally, any effort was done neither to assess the effect of the pH buffer capacity of the feed stream on the removal efficiency nor the need of using a buffer solution. In previous study [18] LLMC was evaluated in counter current and open-loop configuration and three operational parameters: the feed flow rate, the initial ammonia concentration in the water stream, and the pH of solution were evaluated. A 2D numerical model was developed considering advection–diffusion equation inside a single fiber of the lumen with fully developed laminar flow and liquid–gas equilibrium in the membrane–solution interface.[18]

The aim of this work is to study experimentally the use of hydrophobic hollow fiber contactors, as pre- or post-treatment step of a two steps membrane distillation process (as described in Figure 1), to reduce the ammonium concentrations below 1 mg N-NH_4/L. A closed-loop experimental set-up was carried out using a sulfuric acid solution as stripping solution. Ammonium removal was evaluated from aqueous samples simulating the water entering the membrane distillation unit (tap water) and the water produced in the membrane distillation unit (distillated water) (see Figure 1). In both cases the effect of pH on ammonium removal was evaluated. Furthermore, the pH buffer capacity of the aqueous solutions was analysed considering the case of absence of any buffering solution (e.g. distillated water and water with low content of bicarbonate) or aqueous solutions having a pH buffer solution (e.g, a pH buffer close to the pKa of the NH_4^+/NH_3 system). Finally, a numerical algorithm to describe the ammonium removal processes on the HFMC module was developed incorporating the influence of the pH buffer capacity on the removal efficiency. It allowed estimating the experimental conditions where the target requirements of ammonium concentration below 1 mg N-NH_4/L can be achieved to assure water with conductivity lower than 1 µS/cm. Furthermore, the feed pH variation due to the conversion of ammonium to ammonia, with the release a proton ion, was also incorporated by means of acid base reactions.

2. Materials and methods

Ammonium feed solutions were prepared simulating the composition of the two types of potential streams of water purification process for hydrogen production described on Figure 1.

Figure 1.

a) Solutions containing ammonium before being treated by the membrane distillation unit, characterized by the following average composition: Ca^{2+} (54 mg/L), Mg^{2+} (12 mg/L), Na^{+} (15 mg/L), K^{+} (3 mg/L), HCO_3^{-},(170 mg/L), SO_4^{2-} (36 mg/L), NO_3^{-} (4 mg/L), Cl^{-}(34 mg/L). The water composition is approaching the average composition of the surface water.

b) Solutions containing ammonium after being treated with the membrane distillation unit, prepared by using demineralized water.

Experiments were carried out by using the hollow-fiber set-up shown in Figure 2. It consisted on the HFMC module, two peristaltic pumps and two tanks of polypropylene, one for the ammonium solutions and the other for the sulfuric acid solution. All test components were connected by clear PVC flexible tubes. The propylene HFMC module used was a Liquid-Cel 2.5x8" Extra Flow X30HF from Membrane–Charlotte (Celgard, USA). The properties of HFMC are summarized in Table 1.[89]

Table 1.

Figure 2.

Initially, distilled water was passed through the module in order to flush out any traces of compounds from previous experiments. The ammonium feed solutions were pumped through the lumen side of the hollow fiber membrane contactor at different flow rates, while the stripping sulfuric acid solution was circulated into the shell side in a countercurrent mode by using two peristaltic pumps. Both solutions were recirculated to their respective reservoirs. The volumes of the feed and stripping solutions were 10 and 5 L, respectively. At regular time intervals (10 min)

samples (20 mL) were taken from the feeding tank for measuring pH and total ammonium concentration. The receiving tank was not monitored as far as the expected variations on the sulfuric acid concentration were very small due to an imposed excess of acid. At the end of the experiment, the shell and lumen flows were stopped. The system was properly cleaned by passing deionized water through both sides in order to remove the remaining solution.

Experiments were designed at three levels: i) type of water of used, ii) initial ammonium concentration and iii) feed solution pH. Three experiments were performed for each type of water matrix (distilled or tap water) both at each feed ammonium concentration (5-15 mgNH_4^+ /L) and a third one containing a buffer agent, thus modifying the solution pH (7.3-10.4). Finally, the influence of the flow rate was also evaluated by reproducing the conditions of experiment 2 (0.16 L/min) by increasing the flowrate to 0.26 L/min. All tests were carried out at room temperature (22±1°C). Table 2 summarizes the experimental conditions of the performed tests.

Table 2.

Chemicals were analytical grade reagents (Merck, Spain). Ammonium solutions were prepared by dissolving proper amounts of ammonium chloride in 10 L of distilled or tap water for concentrations between 5 and 15 mg/L. pH values of the working solution were adjusted as required by adding NaOH. When the pH of the ammonium solution was desired to be constant along the experiment, a solution of sodium tetraborate (0.3 g of $Na_2B_4O_7{\cdot}10H_20$ /L) was used, otherwise the ammonium chloride solution was prepared by using tap water. The use of a buffer solution of boric/borate mixtures provided a suitable solution in contrast to carbonate/bicarbonate mixtures, since it is not affected by scaling problems and the buffer can be maintained in the system without the necessity of discharge. The stripping solution was prepared dissolving 5 mL of 18 mol/L H_2SO_4 solution into 5 L of distilled water.

The ammonium ion concentration was analysed by an Ion Chromatography System (ICS-1000 Dionex, USA).The pH of the samples was measured with a pH meter (pH meter GLP22 Crison, Spain).

3. Theory

3.1 Ammonium removal mechanism: model description

The mechanism of ammonium ions removal from the feed solution in a HFMC is illustrated on Figure 2. The hydrophobic polypropylene hollow fiber separates both, the feed and the stripping circulating phases and the system is working in closed-loop. The ammonium aqueous phase is fed on the lumen side and the sulfuric acid stripping solution is fed on the on the shell side. An air gap fills the pore of the hydrophobic poly-propylene membrane, which is not wetted by the aqueous solutions. In the first step of the removal process, the ammonia gas form $NH_{3(g)}$ which diffuses from the bulk of the feed stream to the feed–membrane interface. Then, $NH_3(g)$ volatilizes through the feed–membrane interface, and diffuses across the air-filled pore of the membrane, finally, it reacts immediately with sulfuric acid at the membrane interface of the shell side.

Several mathematical models have been developed in previous studies. Wickramasinghe et al.[12] demonstrated that the separation efficiency was controlled by the resistance in the lumen side and determined the mass transfer coefficients of ammonia using different configurations. Moreover, Ashrafizadeh and Khorasani [10] studied the influence of different parameters, such as inlet feed flow, initial concentration, temperature or pH, on the ammonium removal efficiency and optimized the process for a commercial membrane contactor. Furthermore, Tan et al. [13] modeled the removal of ammonia with Polyvinylidene fluoride (PVDF) membrane contactors incorporating the resistance in the feed and membrane phases. Mandowara and Bhattacharya [14] developed a 2D mathematical model for polypropylene (PP) membrane contactors incorporating the effect of pore diffusion and mass transfer resistance and Agrahari et al. [15] developed a model taken into

account the molecular and Knudsen diffusion effects as well as the rates of adsorption and desorption of ammonia molecules to and from the walls of the pores during the transport through the membrane. More recently, Rezakazemi et al. [16] used COMSOL Multiphysics to solve a 2D diffusion model to predict the unsteady state of ammonia transport and Nosratinia et al. [17] to describe the concentration profile inside the membrane.

The algorithm used in this study takes into account unsteady state and isothermal conditions and considers the Henry law applicable in the feed-membrane interface, no pore blockage, the feed aqueous solution do not fills the membrane pores, ammonia reaction with the sulfuric acid solution is instantaneous, the sulfuric concentration on the receiving phase is in excess along the experiment, flow rates of ammonium and sulfuric acid solutions are constant and the feed tank operates at the perfect mixing mode. It integrates the assumptions made by previous studies [14–16,20,21] in one single approach but introducing, as the first time, the effect of the pH buffer capacity of the feed stream. The model was validated by using the experimental data obtained by the membrane contactor set-up.

Then, accordingly the transport of the both ammonia species (as $NH_{3(g)}$) in the lumen is expressed through a convective-diffusive equation:

$$\frac{\partial C_j}{\partial t} + \tilde{U} \cdot \nabla C_j = D_j \nabla^2 C_j + R_j \qquad (3)$$

where C_j is the total ammonium concentration in the feed phase (mol/m^3), D is diffusivity of the component in water (m^2/s), R_j is the ammonia production rate due to chemical reaction defined by equation 1 (mol/s·m^3), U is the velocity vector (m/s).

In this process there is no chemical reaction in the lumen side, additionally to the acid base reaction, and the symmetry assumed inside the lumen is cylindrical. Furthermore, the radial component of velocity also becomes zero [20] as the rate of diffusion of ammonia in water is negligible and the flow is in the Z direction. Then, equation 3 is transformed as follows:

$$\frac{\partial C_j}{\partial t} + U_z \frac{\partial C_j}{\partial Z} = D_j \left[\frac{1}{r} \frac{\partial}{\partial r} \left(r \frac{\partial C_j}{\partial r} \right) + \frac{\partial^2 C_j}{\partial Z^2} \right] \quad (4)$$

The velocity distribution in the fiber under laminar flow conditions can be written as:

$$U_z(r) = \overline{U} \left\{ 1 - \left(\frac{r}{r_{hf}} \right)^2 \right\} \quad (5)$$

where r is radial coordinate (m) and r_{hf} is radius of the fiber. Defining $\overline{U}$ to be the average velocity of the fluid inside the lumen:

$$\overline{U} = \frac{Q}{N \pi r_{hf}^{\ 2}} \quad (6)$$

where Q is the flow rate (m^3/s) and N is the number of fibers in the HFMC. Once defined the equations for the mass balance within fiber, the boundary conditions are defined by:

$$C_{j,Z=0} = C_{\tan k} \quad (7)$$

$$\left(\frac{\partial C_j}{\partial r} \right)_{r=0} = 0 \quad (8)$$

$$-D_j \left(\frac{\partial C_j}{\partial r} \right)_{r=r_{hf}} = k_{g,pore} \left(\frac{p^g{}_{a,\text{int}}}{R_g T} \right) \quad (9)$$

Where, the mass transfer coefficient inside the pore, $K_{g,pore}$ (m/s) is defined by: [21]

$$k_{g,pore} = D_{a,c,pore} \left\{ \frac{\varepsilon}{\tau b} \right\} \quad (10)$$

$D_{a,c,pore}$ is the ammonia diffusivity (m^2/s), ε is porosity of the membrane, b is membrane thickness (m) and τ is tortuosity was calculated through the correlation proposed by Bottino et al. [22] and Mandowara and Bhattacharya:[14]

$$\tau = \frac{1}{\varepsilon^2} \quad (11)$$

The diffusivity of gaseous ammonia ($NH_{3(g)}$) in the pore is calculated by:

$$\frac{1}{D_{a,c,pore}} = \frac{1}{D_{k,a,pore}} + \frac{1}{D_{a,air}} \quad (12)$$

where $D_{k,a,\ pore}$ is the Knudsen diffusion (m^2/s), $D_{a,air}$ is the ammonia diffusivity in the air (m^2/s). The Knudsen diffusion was calculated by:

$$D_{k,a,pore} = \frac{d_{pore}}{3}\left(\frac{8R_gT}{\pi M_a}\right)^{1/2} \quad (13)$$

where d_{pore} is diameter of pore (m), R_g is the universal gas constant (J/mol·K), T is the temperature (K) and M_a is the molecular weight of ammonia (g/mol).

The total ammonium concentration (C_j) (mol/m^3) in the aqueous solution is calculated by:

$$C_j = [NH_3] + [NH_4^+] \quad (14)$$

where both concentrations could be estimated by using the acid dissociation constant $K_a(T)$ (NH_4^+/NH_3).

$$K_a(T) = \frac{[NH_3][H^+]}{[NH_4^+]} \quad (15)$$

On the other hand, at the liquid (feed phase)-gas (porous phase) interface, Henry's law may be applied: [15]

$$P^g_{a\,int} = H^T_a [NH_3]_{int} \quad (16)$$

H^T_a is Henry's constant ($Pa \cdot m^3/mol$) and $[NH_3]_{int}$ is concentration of ammonia at liquid-gas interface (mol/m^3).

The temperature dependence of $K_a(T)$ and H^T_a could be described by Montes et al.: [23]

$$K_a(T) = 10^{0.05-2788/T} \quad (17)$$

$$H_a{}^T = \left[\left(\frac{0.2138}{T}\right) * 10^{6.123-1825/T}\right] * R_gT \quad (18)$$

Then, a mass balance for the (NH_4^+/NH_3) system in the tank under the assumption of uniform mixing can be written: [14]

$$V\frac{dC_{\tan k}}{dt} = Q(C_{j,z=L} - C_{\tan k}) \quad (18)$$

Where at the initial condition, at t= 0:

$$C_0 = C_{\tan k} \quad (19)$$

For a closed-loop system, recirculation is taken into account as a global mass balance equation and the concentration in the tank could be described by Eq. 18.

The variation of pH in the feeding tank, assuming fast acid-base reactions, can be described following the method proposed by Gustafsson et al. [24] For a solution containing monoprotic acids (a_i) and bases (b_j) and taking into account both mass and the electro-neutrality balances, the pH of the solution can be calculated by solving Eq. 20:

$$0 = \frac{K_W}{10^{-pH}} - 10^{-pH} + \sum C_{a,i}\frac{K_{a,i}}{10^{-pH}+K_{a,i}} - \sum C_{b,j}\frac{10^{-pH}}{10^{-pH}+K_{b,j}} \quad (20)$$

where $C_{a,i}$ and $C_{b,j}$ are the concentrations of the acids and bases respectively and $K_{a,i}$ and $K_{b,j}$ are the acidity and basicity constants of the monoprotic acid and base respectively.

The pH buffer capacity (β) of solutions containing weak acid-base protolytes can be obtained by differentiating Eq. 21.

$$\beta = \frac{dC_b}{dpH} = 2.303*\left(\frac{K_W}{10^{-pH}} + 10^{-pH} + \frac{10^{-pH}C_aK_a}{(K_a+10^{-pH})^2}\right) \quad (21)$$

The pH buffer capacity expresses how sensitive is the buffer concentration (C_b) to pH variations. The initial concentration of the species $C_{a,i}$ and $C_{b,j}$ could be determined from the initial measured pH .

3.2 Numerical solution of the algorithm

Simulation of ammonia mass transport inside the lumen was performed using Computational Fluid Dynamic (CFD) techniques based on the finite element method. All the equations describing the separation process with their appropriate boundary conditions were solved using COMSOL

Multiphysics version 4.2a. The equations system was solved with parallel direct linear solver (PARDISO) with a relative tolerance of 0.001. Under these conditions the solver is well suited for solving stiff and non-stiff non-linear boundary value problems. Adaptive mesh refinement in COMSOL, which generates the best and minimal meshes, was used to mesh the HFMC geometry. A refinement on the mesh near to the membrane surface was implemented for all the calculations. A mass balance in the tank was introduced as a global equation for each chemical species in order to define their concentration change with time. The structure of the developed algorithm for the numerical simulation is shown in Figure 3. A Dell-PC-Intel core 2 (CPU speed is 3 GHz) was used to solve the sets of equations. By this method, variations of both concentration and pH can be evaluated in the feeding tank.

Figure 3.

4. Results and discussion

4.1. Removal of ammonium in un-buffered pH aqueous solutions

The pH variation in the feeding tank for the experiments described in Table 2 (for non-buffered solutions) is shown in Figure 4. As can be seen, the pH of the feed circuit decreases due to the release of equimolecular number of proton ions by mole of ammonium ions transported from the feed to the stripping solution as it is described by equation 1 (acid-base reaction).

Figure 4.

Figures 4a and 4b show pH and ammonium changes as a function of time, respectively, along the experimental test. The removal efficiency of NH_4^+ from solutions prepared with distilled water (simulating the water produce from the membrane distillation unit in Figure 1) shown values below 15%, although the pH of initial solution is increased up to 9.3 by addition of a small amount of NaOH, basically due to the decrease of the pH measured in the feed tank up to values around

7.2 where the dominant species (>99%) in aqueous solution is NH_4^+ instead of NH_3. For such low pH values the acid-base equilibrium is shifted to the ammonium form and then the concentration of free ammonia in solution and ammonia gas are reduced strongly at the solution/membrane interface, decreasing the flux trough the membrane. Contrary, in the presence of a $3x10^{-3}$ mol/L of HCO_3^-/CO_3^{2-} at pH=9.8, typically present in the inlet effluents of the membrane distillation treatment unit, the buffering capacity of the mixture, was able to control the reduction of the pH of the feed solution from 9.8 to 8.8 and the removal of ammonium was increased up to 60%. In the pH range (9.8 to 8.8) the molar ratio NH_3/NH_4^+ ranges from 2 to 0.1 however still the system is able to extract 60% of the total ammonium concentration. Similar ammonium removal behaviour was reported by Tan et al. [13] using a PVDF hollow fiber membrane at pH values between 8 and 12, however the ammonium concentration was evaluated between 140 and 754 mgNH_4^+/L.

Also Ashrafizadeh et al. [10] studied the transport of NH_4^+ from 50 to 800 mgNH_4^+/L as a function of pH, between 8 to 13, using a HFLLC module similar to that used in this work, nonetheless, the changes of pH in the feed stream were not reported. For the experiments at low pH values, where the buffer capacity will be the lowest, the ammonium removal extraction decreased up to 50-60%.

The removal process is controlled mostly by the chemical equilibrium of the system $NH_4^+/NH_3/NH_3(g)$, which highly depends on the pH. The change of the pH of the feed solution, typically not addressed in the modelling of this system, could be described by integration of the acid-base balance of the system (Eq. 20) into the algorithm. As can be seen in Figure 4b measured pH values (symbols) are well predicted by the extended model (solid lines), in view of the small deviations observed between them.

Taking into account that only $NH_{3(g)}$ is transported from the lumen to the shell side trough the membrane contactor, the chemical equilibrium modifies the pH (Equations 1-2), and in turn, a new concentration of species at the end of the contactor is established. Therefore, calculating the proton balance in the tank in a similar way described by Eq. 18, the new distribution of species is

determined and a new pH of the feed solution can be calculated. None of the studies on modelling ammonium removal from aqueous solutions by hollow fibre membrane contactors have included the influence of the pH buffer capacity on the feed solutions.

As can be seen in experiments performed with distillated water or water containing HCO_3, the pH of the feed solution decreases from initial pH values (around 9.3 to 10.5) up to below 9 depending on the experiment conditions, indicating low pH buffer capacity, which in the case of the distilled water the buffer capacity it is associated only to the presence of ammonium ions and in the case of solution prepared with tap water it is associated to the presence of bicarbonate.

Figure 5.

In Figure 5a the ammonia-ammonium equilibrium as function of pH and buffer capacity of the acid-base system present on the model solutions (NH_4^+/NH_3), ($H_2CO_3/(HCO_3^-/CO_3^{2-})$ is shown. As it can be seen, the buffer capacity of the ($H_2CO_3/HCO_3^-/CO_3^{2-}$) system have two maximum around 6.3 (pka1) and 10.3 (pKa2), however the concentration of HCO_3^- and pH of the raw water on the membrane distillation provides a reduced buffering capacity as it shown in the case of the experiment with the initial pH of 10.3, where the pH decreases up to 9.0 Then, even for low levels of ammonium concentrations (5-15 mg NH_4^+/L) a decrease up to 2 units of pH was observed. In a first attempt, the use of HCO_3^-/CO_3^{2-} as pH buffering solution was discarded, due to its reduced buffer capacity at the expected conditions, and additionally the potential transformation to H_2CO_3 and finally $CO_2(g)$ forms that could be transported through the membrane pores, then reducing the buffer capacity. Additionally, the increase of carbonate, bicarbonate ions is not appropriate as could promote scaling problems with Ca(II) and Mg(II) ions by precipitation of $CaCO_3$ or $MgCO_3$.

4.2 Removal of ammonium in buffered pH aqueous solutions

One possibility to reduce the pH variation due to the release protons by the ammonium removed is the use of a buffer solution. In most of the published studies Tan et al., [13] Asrafizadeh et al., [10] Hasanoglu et al. [27] the pH of the feed solution was typically buffered by NaOH solutions to reach values from 11 to 13. As described, previously the possibility of using bicarbonate buffers and using a strong base (e.g. NaOH) to reach the pKa_2 (HCO_3^-/CO_3^{2-}) was discarded initially to avoid scaling problems and it was selected as buffer solution boric/borate (H_3BO_3/ $H_3BO_2^-$) with a pKa (9.2) [6] close to pKa(NH_4^+/NH_3) and working in the upper limit of the buffer solution pH 10 to 10.3. In Figure 5b the ammonia-ammonium equilibrium as function of pH and buffer capacity of the acid-base system present on the model solutions (NH_4^+/NH_3), ($H_3BO_3/(H_2BO_3^-$) is shown.

Figure 6.

Figures 6a and 6b show the ammonium and pH evolution for buffered solutions using boric/borate buffer. The removal efficiency of NH_4^+ reached values higher that 95% with both solutions prepared using distilled water and water containing the HCO_3^-/CO_3^{2-} mixtures. For all the conditions evaluated with initial pH between 10 to 10.5, the final pH was always maintained above pH 9.8, where the molar ratio NH_3/NH_4^+ it is higher than 7, then favouring the transport of NH_3. As can be seen in Figure 6a measured pH values (symbols) are well predicted by the completed model (solid lines), in view of the small deviations observed between them.

In Figure 6b the evolution of the C/C_0 ammonium concentration ratios in the tank as a function of time for buffered solutions with pH values between 10 and 10.5 under different experimental conditions (Table 2) and the model predicted values are also shown. In the case of experiment 7 the flow rate was increased but as can be seen on Figure 6b, the ammonium removal was lower due to the lower effective pH (see Figure 6a).

Semmens et al. [11] studied the influence of pH on the mass transfer of ammonia in highly buffered solutions and demonstrated that only affects the membrane mass transfer but not the feed to membrane transfer. However, Zhu et al. [26] working with unbuffered solutions quantified the influence of pH variations on the feed stream and a mass transfer coefficient dependent on the free ammonia concentration was proposed. A sensitivity analysis to evaluate the effect of the initial concentration, pH and flow rate will be discussed through the model simulation.

Figure 7.

The buffering capacity of the boric/borate and bicarbonate/carbonate mixtures was compared by using the develop algorithm and the evolution of the pH in an ammonium extraction experiment with 15 mgNH_4/L of ammonium is described in Figure 7a. As it could be seen the evolution of pH for both solutions shows an initial drop from 10.4 to 10.2 and 10.1, for the carbonate/bicarbonate and the boric/borate buffers respectively, and after the pH kept constant as the extraction process proceeds. Then, although using higher pH will favour the extraction process, the use of boric/borate buffer solutions to maintain the pH above 10, is providing a suitable solution. The variation of the ammonium extraction (C/C_0) for both buffered solutions (Figure 7b shown the same profile with time). Then the use of the boric/borate buffer is recommended in front of the carbonate/bicarbonate buffers to avoid scaling problems.

The removal of ammonium traces would be only efficient if it is performed under constant and controlled pH, and the use of liquid-liquid contactors will only provide suitable removal performances, in the water purification step using membrane distillation processes, if developed as pre-treatment step.

4.3 Numerical simulation

The 2D model was used to describe the concentration of total ammonium in the tank. The mathematical algorithm was used to predict the performance of the process under different

conditions which are summarized Table 3, and results are shown in Figure 8. According to Figure 8a and 8b the ammonium removal efficiency by HFMC is improved by raising the pH or the flow rate. This is in agreement with the results found by Qu et al. [25] and Agrahari et al.[15] According to them, the feed pH value was proved to be the most dominant factor and the optimal feed pH was found around 12. This can be explained with the pH equilibrium diagram (Figure 5), in which at such pH the hydroxyl ions become dominant, it results in a system with high buffer capacity.

Table 3.

Figure 8.

The case of the flow rate influence corresponds to the contribution of convective mass transfer in the lumen side. Figure 8b indicates that increasing flow rate decreases ammonia concentration in the feeding tank leading to an increase in the ammonia removal. For a single pass (open loop regime), increasing flow rate causes that residence time of feed phase in the tube side to be lower, nevertheless at larger flow rates, the number of times that the liquid in the tank passes through the membrane contactor increases. Therefore, increasing flow rate or feed velocity is favourable for ammonia removal in membrane contactors.

The influence of the initial ammonium concentration was also studied. It should be mentioned that according to Mandowara and Bhattacharya [14], the evolution of the ammonium concentration is independent of the initial concentration in the feed tank. However, once the pH is dependent of the concentration of ammonium, the variation of the pH is proportional to the removal amount of ammonia. This variation is predicted by the model as is shown in Figure 9. In this figure the ammonium removal (C/C_0) was predicted for three different initial concentrations (2, 5 and 10 mg/L) and the ammonium removal profile reported a not significant difference between 2 and 5 mg/L and slight deviation between 5 and 10 mg/L. Similar modelling results were described by

Agrahari et al.[15] who studied the various transport steps associated with the degasification of NH_3 from water using a HFMC. The removal rate was shown to be dependent on the solution pH however, the initial NH_3 concentration was in the range of 200–1500 mgNH_4^+/L and removal efficiency was found to be 99% or higher under the different operating conditions selected.

Figure 9.

4.4. Prediction of concentration profiles distribution of ammonia in the lumen

The model was also used to determine the concentration distribution in the feed stream of the membrane contactor. Figure 10 show the concentration profiles of ammonium in the feed stream of the membrane contactor. The ammonium aqueous feed solution enters, from the bottom part (z = 0). As the feed passes through the hollow fiber, due to the concentration gradient, ammonium is transferred from the bulk of the feed toward the feed–membrane surface. At the surface of the membrane, only ammonia evaporates into the membrane pores and reaches the shell side. Figure 10a-c shows the evolution of the concentration ratio C/C_0 as a function of the fiber radius and as a function of the fiber length for experiments for buffered solutions at pH (8.3, 9.3 and 10.3). As could be seen at pH values of 10.3 (pH=pKa+1) the concentration gradient as a function of the radii, decreases, as the solution moves along the fiber and for values of Z=L (end of the fiber) the minimum concentration gradient is measured due to the reduction of ammonium concentration ratios between 0.5 and 0.6. Contrary, for the simulation with pH=9.3, reduction of ammonium concentration ratios ranged between 0.9 and 0.75, and for pH=8.3, where the ammonium form is predominant in solution in comparison to ammonia, the reduction of the concentration ratio at the exit of the fiber is higher than 0.90, indicating removal values of ammonium below 5-10%. This concentration profiles as a function of pH, provides a good description of the effect of pH on the ammonium removal, when the feed solution losses its pH buffer capacity reaching values below the pKa value of the ammonium/ammonia system.

Figure 10.

Mandowara and Bhattacharya [14] reported a decrease in ammonia concentration along the radial and axial directions on simulation studies of ammonia removal using a similar hollow fibre membrane contactor. The radial diffusion and convection in the lumen side were identified as responsible for this effect, and demonstrated that axial diffusion was not significant compared to the radial diffusion. As demonstrated in this work, pH up to 10.5 increased the fractional removal and beyond this value the increase of pH is associated with a limited increase on the removal efficiency.

The numerical code could be use also used to study the variations of the radial ammonium concentration in the feed fiber side of the membrane contactor. Figure 11 provides the radial concentration profile at different axial positions along the feed fiber side (e.g. for different cross section values in the z-axial coordinate within the fiber length L). In the region near the axis of the fiber, e.g. r = 0 the bulk ammonium concentration slightly changes. The maximum concentration of ammonium can be observed in the center of the fiber due to axial symmetry assumption. Concentration of ammonium decreases gradually in the region between the center and wall of the feed fiber side. Eventually, in the region adjacent the membrane–feed interface, concentration sharply decreases. This type of profiles is attributed to the formation of the concentration boundary layer near the fiber wall. On the other hand, at the axial positions near the fiber in-let, e.g. Z = 0, the concentration is constant. Efforts on ammonia removal modelling by HFLC have been reviewed by Kumar and Sastre [28] showing similar prediction for the variation of concentrations in both the axial and radial directions.

Figure 11.

5. Conclusions

The hollow fiber membrane contactor technology is a suitable solution to remove low levels of ammonium from raw water used to feed membrane distillation treatment in order to produce suitable water quality (e.g. conductivity lower than 1 μS/cm) for further electrolysis. Residual levels below 1 mg NH_4^+/L allow achieving the quality requirements. The effect of the feed stream pH and the possibility to use a pH buffer solution was thoroughly studied in order to describe its influence during the process and it was included in a mathematical model by coupling acid-base reactions to the mass balance equations. The ammonium removal efficiency by HFMC was improved by raising the pH or the flow rate. On the other hand, due to the low pH buffer capacity of the raw water (low concentration of bicarbonate), the ammonia concentration requirements were reached only when a buffer agent was added to the working solution. This cleaner production approach of water purification is based on a closed loop configuration, which allows maintaining all chemical compounds in the system without the necessity of discharge. The results obtained in this study, can be used to evaluate the hollow fiber membrane contactors performance for ammonia removal from aqueous solutions under different processing conditions and to define the operational parameters necessary to operate efficiently.

List of symbols

A membrane surface area (m^2)

b is membrane thickness (m)

$C_{a,i}$ and $C_{b,j}$ are the concentrations of the acids and bases respectively (mol/m^3)

C_b is the buffer concentration

C_j the total ammonium concentration in the feed phase (mol/m^3)

C_{tank} is the concentration in the feeding tank at any moment.

$D_{a,air}$ is the ammonia diffusivity in the air (m^2/s)

$D_{a,c,pore}$ is the ammonia diffusivity (m^2/s),

Dj diffusivity of the component j in water (m^2/s)

$D_{k,a,\ pore}$ is the Knudsen diffusion (m^2/s)

d_{pore} is diameter of pore (m)

H^T_a is Henry's constant ($Pa \cdot m^3/mol$)

K_a ammonium acid dissociation constant

$K_{a,i}$ and $K_{b,j}$ are the acidity and basicity constants of the monoprotic acid and base respectively

$K_{g,pore}$ the mass transfer coefficient inside the pore (m/s)

L length of the hollow fibers (m)

M_a is the molecular weight of ammonia (g/mol)

N is the number of fibers in the HFMC

$[NH_3]$ the equilibrium concentrations of ammonia in the feed solution (mol/m^3)

$[NH_{3(g)}]$ the equilibrium concentration of ammonia at initial time in the bulk feed ($mg\ L^{-1}$)

$[NH_4^+]$ the equilibrium concentrations of ammonium in the feed solution (mol/m^3)

$P^g_{a\ int}$ is the partial pressure of the ammonia at the interface (Pa)

Q is the flow rate (m^3/s)

R the removal efficiency of ammonia (%)

R_j the ammonia production rate due to chemical reaction defined by eq. 1 ($mol/s \cdot m^3$),

r radial coordinate (m)

R_g is the universal gas constant ($J/mol \cdot K$),

r_{hf} radius of the fiber (m)

T is the temperature (K)

U the velocity vector (m/s)

$\overline{U}$ average velocity(m/s)

V volume (m^3)

β the buffer capacity

ε is porosity of the membrane,

τ is tortuosity

Acknowledgments

This study has been supported by the Waste2Product project (CTM2014-57302-R) financed by Ministry of Science and Innovation and the Catalan government (project ref. 2014SGR050). The work of Edxon Eduardo Licon Bernal was supported by the National Council of Science and Technology of Mexico (CONACYT) within the scope of fellowship reg: 213775. The authors also thank to A. Gali, E. Larrotcha and E. Marzo, project leaders of the Greenlysis project from CETaqua, for their support and help during the performance of this study.

References

1. Ursua A, Gandia LM, Sanchis P. Hydrogen Production From Water Electrolysis: Current Status and Future Trends. *Proc IEEE*.100(2):410-426 (2012). doi:10.1109/JPROC.2011.2156750.
2. Marzo E, Gali A, Lefevre B, et al. Hydrogen and Oxygen Production using Wastewater Effluent Treated with Ultra-Filtration and Membrane Distillation (Greenlysis). *Procedia Eng*.44:1744-1746 (2012). doi:10.1016/j.proeng.2012.08.932.
3. Miladinovic N, Weatherley LR. Intensification of ammonia removal in a combined ion-exchange and nitrification column. *Chem Eng J*. 135(1-2):15-24 (2008). doi:10.1016/j.cej.2007.02.030.
4. Sarioglu M. Removal of ammonium from municipal wastewater using natural Turkish (Dogantepe) zeolite. *Sep Purif Technol*. 41(1):1-11 (2005). doi:10.1016/j.seppur.2004.03.008.
5. Gabelman A, Hwang ST. Hollow fiber membrane contactors. *J Memb Sci*. 159(1-2):61-106 (1999). doi:10.1016/S0376-7388(99)00040-X.

6. Li J-L, Chen B-H. Review of CO2 absorption using chemical solvents in hollow fiber membrane contactors. *Sep Purif Technol*. 41(2):109-122 (2005). doi:10.1016/j.seppur.2004.09.008.

7. Shirazian S, Moghadassi A, Moradi S. Numerical simulation of mass transfer in gas–liquid hollow fiber membrane contactors for laminar flow conditions. *Simul Model Pract Theory*. 17(4):708-718 (2009). doi:10.1016/j.simpat.2008.12.002.

8. Iversen SB, Bhatia VK, Dam-Johansen K, Jonsson G. Characterization of microporous membranes for use in membrane contactors. *J Memb Sci*. 130(1-2):205-217(1997). doi:10.1016/S0376-7388(97)00026-4.

9. Latimer WM. *Reference Book of Inorganic Chemistry*. (1951).

10. Ashrafizadeh SN, Khorasani Z. Ammonia removal from aqueous solutions using hollow-fiber membrane contactors. *Chem Eng J*. 162(1):242-249 (2010). doi:10.1016/j.cej.2010.05.036.

11. Semmens MJ, Foster DM, Cussler EL. Ammonia Removal from Water Using Microporous Hollow Fibers. *J Memb Sci*. 51(1-2):127–40 (1990).

12. Wickramasinghe SR, Semmens MJ, Cussler EL. Mass transfer in various hollow fiber geometries. *J Memb Sci*. 169(3):235-250 (1992). doi:10.1016/0376-7388(92)80042-I.

13. Tan X, Tan SP, Teo WK, Li K. Polyvinylidene fluoride (PVDF) hollow fibre membranes for ammonia removal from water. *J Memb Sci*. 271(1-2):59-68 (2006). doi:10.1016/j.memsci.2005.06.057.

14. Mandowara A, Bhattacharya PK. Simulation studies of ammonia removal from water in a membrane contactor under liquid-liquid extraction mode. *J Environ Manage*. 92(1):121-130 (2011). doi:10.1016/j.jenvman.2010.08.015.

15. Agrahari GK, Shukla SK, Verma N, Bhattacharya PK. Model prediction and experimental studies on the removal of dissolved NH3 from water applying hollow fiber membrane contactor. *J Memb Sci*. 390-391:164-174 (2012). doi:10.1016/j.memsci.2011.11.033.

16. Rezakazemi M, Shirazian S, Ashrafizadeh SN. Simulation of ammonia removal from industrial wastewater streams by means of a hollow-fiber membrane contactor. *Desalination*. 285:383-392 (2012). doi:10.1016/j.desal.2011.10.030.

17. Nosratinia F, Ghadiri M, Ghahremani H. Mathematical modeling and numerical simulation of ammonia removal from wastewaters using membrane contactors. *J Ind Eng Chem*. 20(5):2958-2963 (2014). doi:10.1016/j.jiec.2013.10.065.

18. Licon E, Reig M, Villnova P, Valderrama C, Gibert O, Cortina JL. Ammonium removal by liquid–liquid membrane contactors in water purification process for hydrogen production. *Desalin. Water Treat. (*2014); doi: 10.1080/19443994.2014.974216.

19. Fouad EA, Bart H-J. Emulsion liquid membrane extraction of zinc by a hollow-fiber contactor. *J Memb Sci*. 307(2):156-168 (2008). doi:10.1016/j.memsci.2007.09.043.

20. Mansourizadeh A, Ismail AF. Hollow fiber gas-liquid membrane contactors for acid gas capture: a review. *J Hazard Mater*. 171(1-3):38-53 (2009). doi:10.1016/j.jhazmat.2009.06.026.

21. Mandowara A, Bhattacharya PK. Membrane contactor as degasser operated under vacuum for ammonia removal from water: A numerical simulation of mass transfer under laminar flow conditions. *Comput Chem Eng*. 33(6):1123-1131 (2009). doi:10.1016/j.compchemeng.2008.12.005.

22. Bottino A, Capannelli G, Comite A, Felice RD, Firpo R. CO2 removal froma gas stream by membrane contactor. *Sep Purif Technol*. 59: 85-90 (2008).

23. Montes F, Rotz CA, Chaoui H. Process Modeling of Ammonia Volatilization from Ammonium Solution and Manure Surfaces: a Review with Recommended Models. *Trans Asabe*. 52(5):1707-1719 (2009).

24. Gustafsson TK, Skrifvars BO, Sandström K V., Waller K V. Modeling of pH for control. *Ind Eng Chem Res*. 34(3):820-827 (1995).

25. Qu D, Sun D, Wang H, Yun Y. Experimental study of ammonia removal from water by modified direct contact membrane distillation. *Desalination*. 326:135-140 (2013). doi:10.1016/j.desal.2013.07.021.

26. Zhu Z, Hao Z, Shen Z, Chen L. Modified modeling of the effect of pH and viscosity on the mass transfer in hydrophobic hollow fiber mebrane contactors, *J Memb Sci*. 250: 269–273 (2005).

27. Hasanoglu A, Romero JB, Pérez B, Plaza A. Ammonia removal from wastewater streams through membrane contactors:Experimental and theoretical analysis of operation parameters and configuration, *Chem Eng J*. 160: 530:537 (2010).

28. Kumar AP, Sastre AM. State-of-the-art review on hollow fibre contactor technology and membrane-based extraction processes. *J Memb Sci*. 430: 263–303 (2013).

Table 1. Properties of polypropylene hollow fiber membrane contactor (PP-HFMC) module used for ammonia removal.

Membrane contactor property	Typical values
Porosity (%)	40
Effective Pore Size (μm)	0.03
Burst Strength (PSI (15.5 kg/cm^2))	220
Tensile Break Strength (g/filament)	175
Resistance to Air Flow (Gurley s)	25-45
Shrinkage, Axial Direction (%)	5
Inner diameter of the lumen (μm)	240
Wall Thickness (μm)	30
Outer diameter of the lumen (μm)	300
Number of fibers, N (m)	9950
Effective length of the fiber, L (m)	0.15
Packing fraction	0.26
Pore diameter, d_{pore} (m)	3×10^{-8}
Thickness of the membrane, b (m)	3×10^{-5}
Tortuosity of pore, τ	2.25
Shell diameter d_s (m)	0.063
Fiber bundle diameter d_a (m)	0.047
Distribution tube diameter d_D (m)	0.022

Table 2. Experimental conditions for ammonia removal by HFMC.

Experiment	C_0 (mg NH_4^+/L)	Q (L/min)	$Na_2B_4O_7 \cdot 10H_20$ (g/L)	Type of water	pH_0
1	5	0.263	-	Tap	7.3
2	15	0.263	0.3	Distilled	10.3
3	15	0.263	-	Distilled	9.3
4	5	0.263	0.3	Distilled	10.4
5	15	0.263	-	Tap	9.8
6	15	0.263	0.3	Tap	10.2
7	15	0.612	0.3	Distilled	10.1

Table 3. Experimental conditions simulated by the model for ammonia removal from aqueous solution by HFMC.

Simulation	pH	Q (m^3/s)	C_0 (mg/l)
1a	7	$4.39x10^{-6}$	15
2a	8	$4.39x10^{-6}$	15
3a	9	$4.39x10^{-6}$	15
4a	10	$4.39x10^{-6}$	15
5a	11	$4.39x10^{-6}$	15
1b	10.3	$6.6x10^{-6}$	15
2b	10.3	$2.49x10^{-5}$	15
3b	10.3	$3.72x10^{-5}$	15
4b	10.3	$4.94\ x10^{-5}$	15
5b	10.3	$6.16\ x10^{-5}$	15

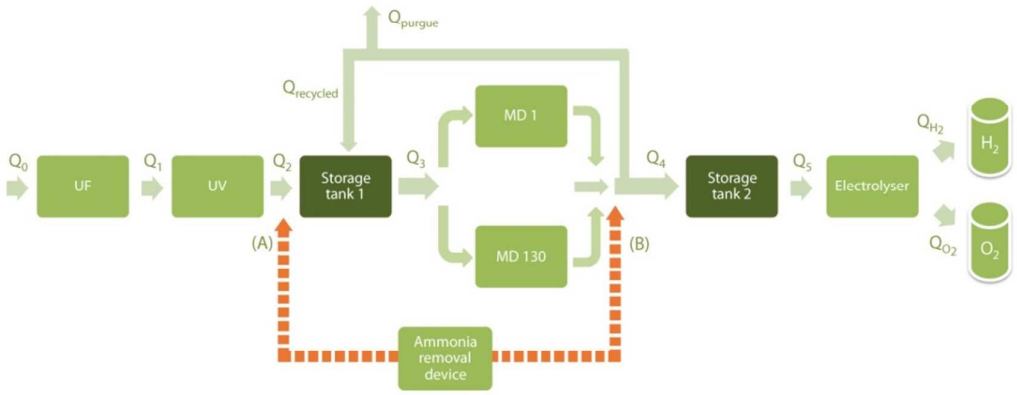

Figure 1. Schematic representation of the hydrogen production by electrolysis in the Greenlysis project

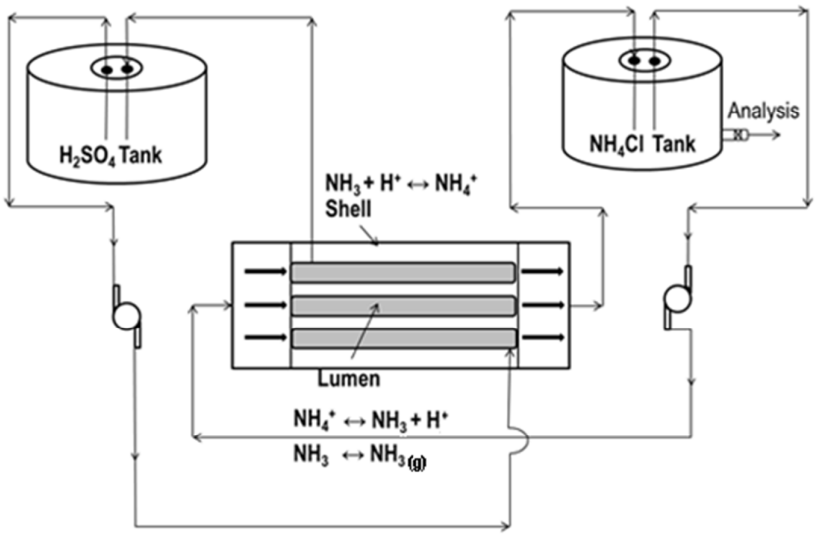

Figure 2. Membrane contactor operated in close loop regime for removal of dissolved ammonium

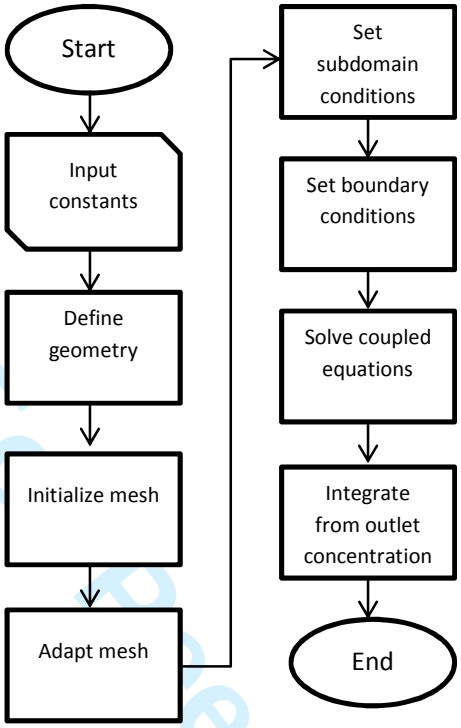

Figure 3. Structure of the algorithm developed for the numerical simulation of ammonium removal from aqueous solutions

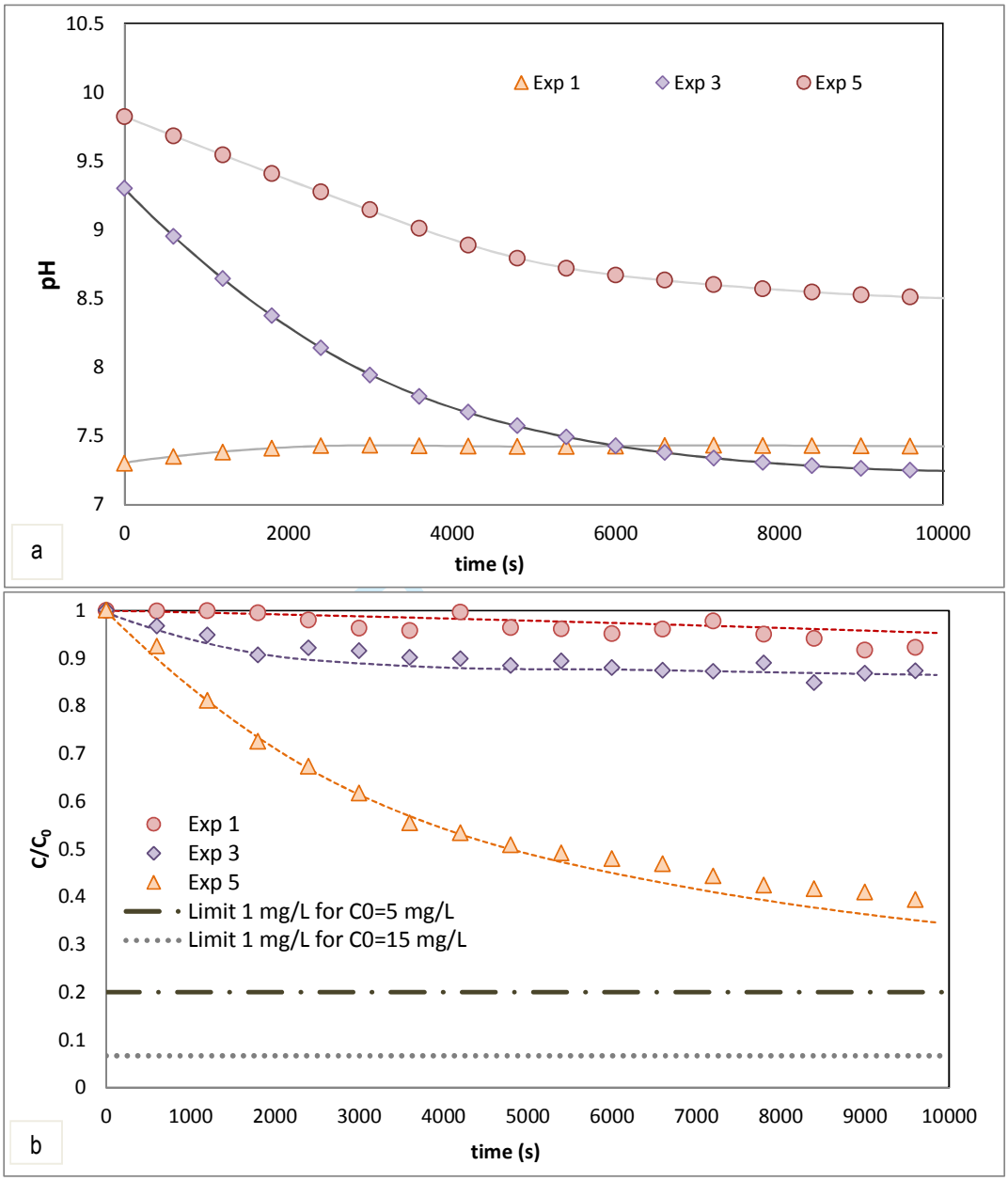

Figure 4. a) Evolution of pH in the ammonium removal by HFMC experiments and theoretical curves. b) Comparison between the concentration evolution and the predicted values by the numerical simulation for the experiments 1, 3 and 5

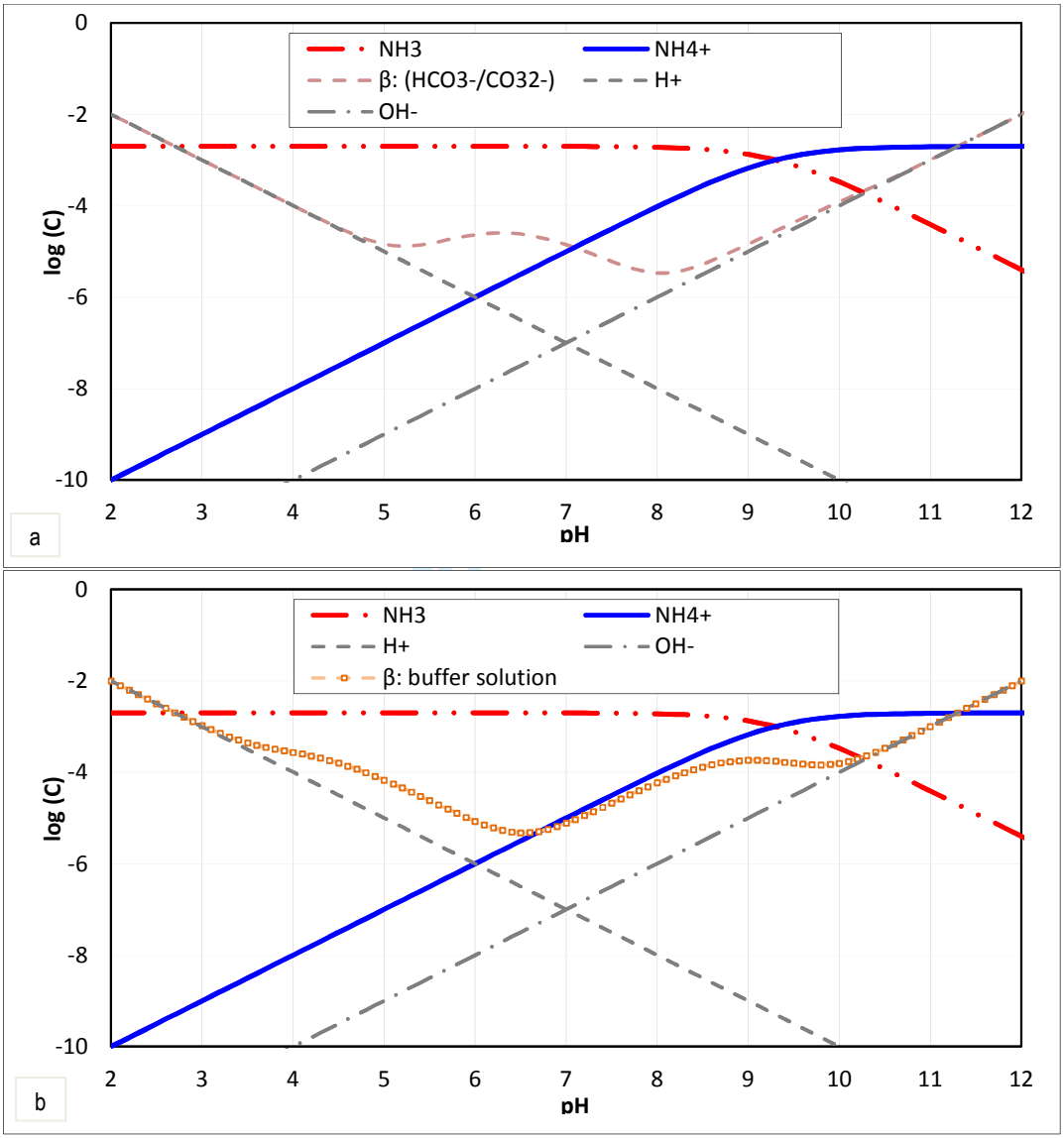

Figure 5. Ammonia-ammonium equilibrium as function of pH with the buffer capacities (β) of a) just carbonate HCO_3^-/CO_3^{2-} and b) the buffer solution

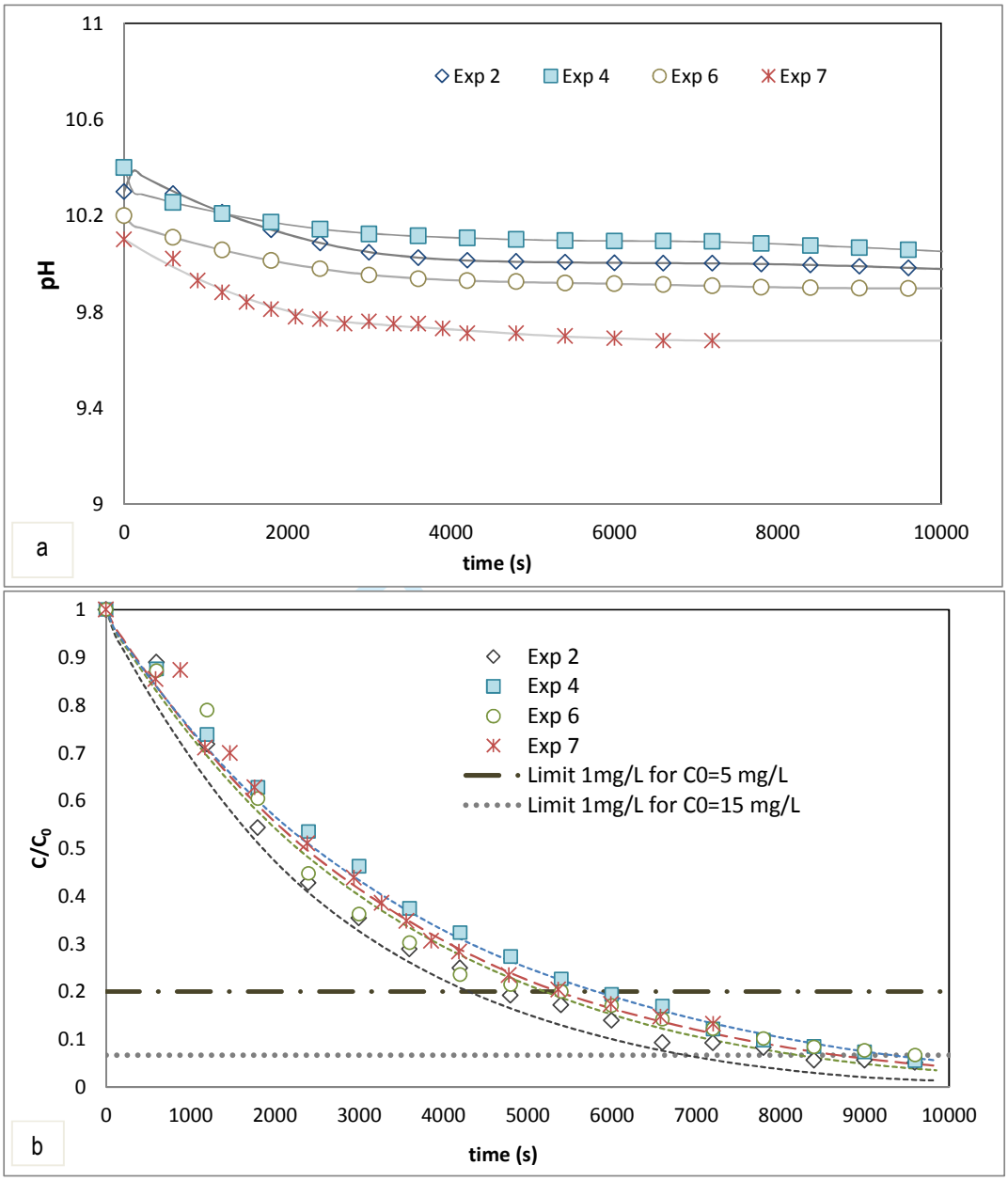

Figure 6. a) Evolution of pH in the feeding tank. b) Comparison between the experimental concentration evolution and the predicted values by the numerical simulation for the experiments 2, 4, 6 and 7

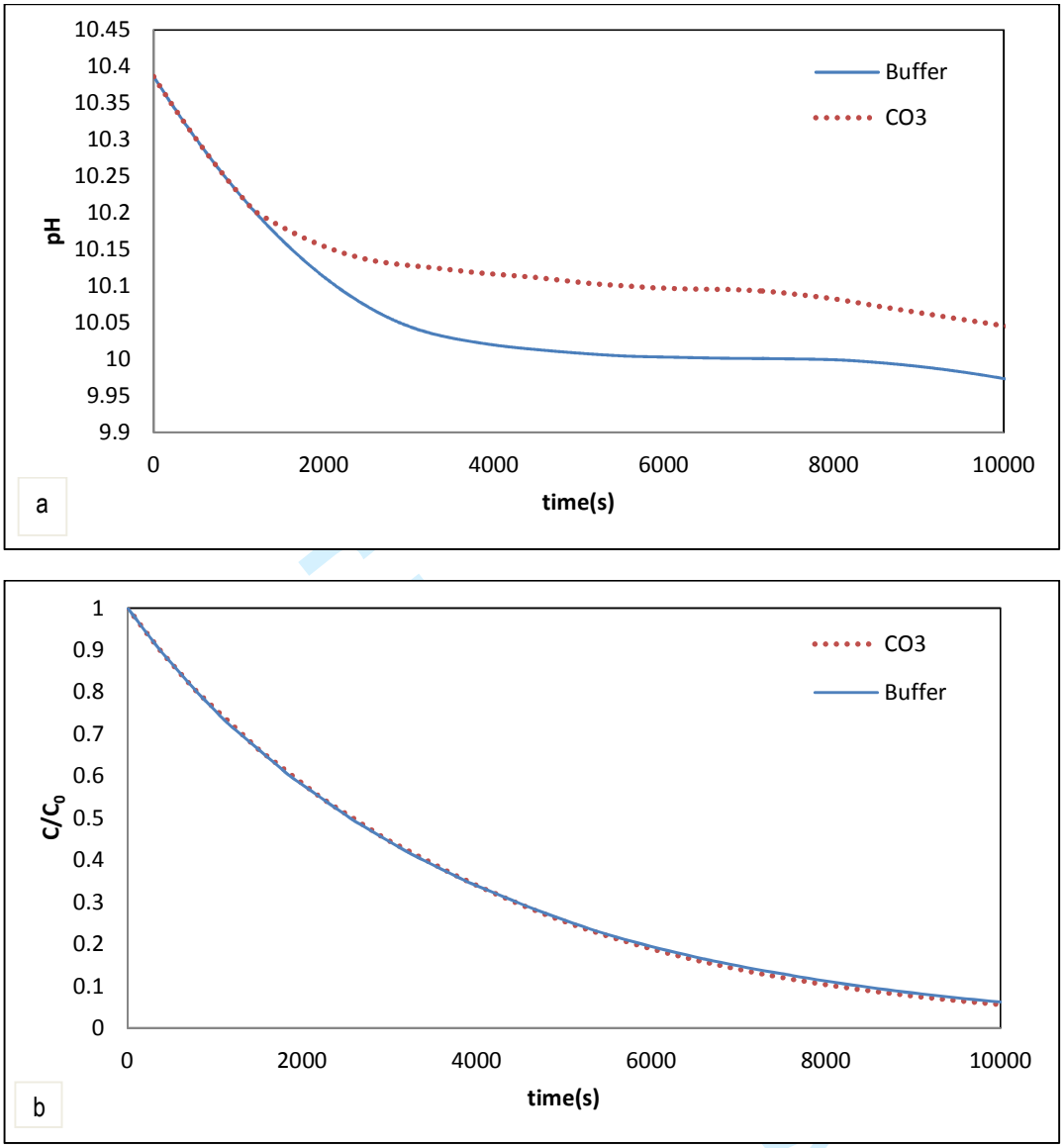

Figure 7. a) Evolution of the pH considering the use of a buffer solution or (HCO_3^-/CO_3^{2-}) to maintain the pH and their corresponding concentration evolution estimated by numerical simulation (b)

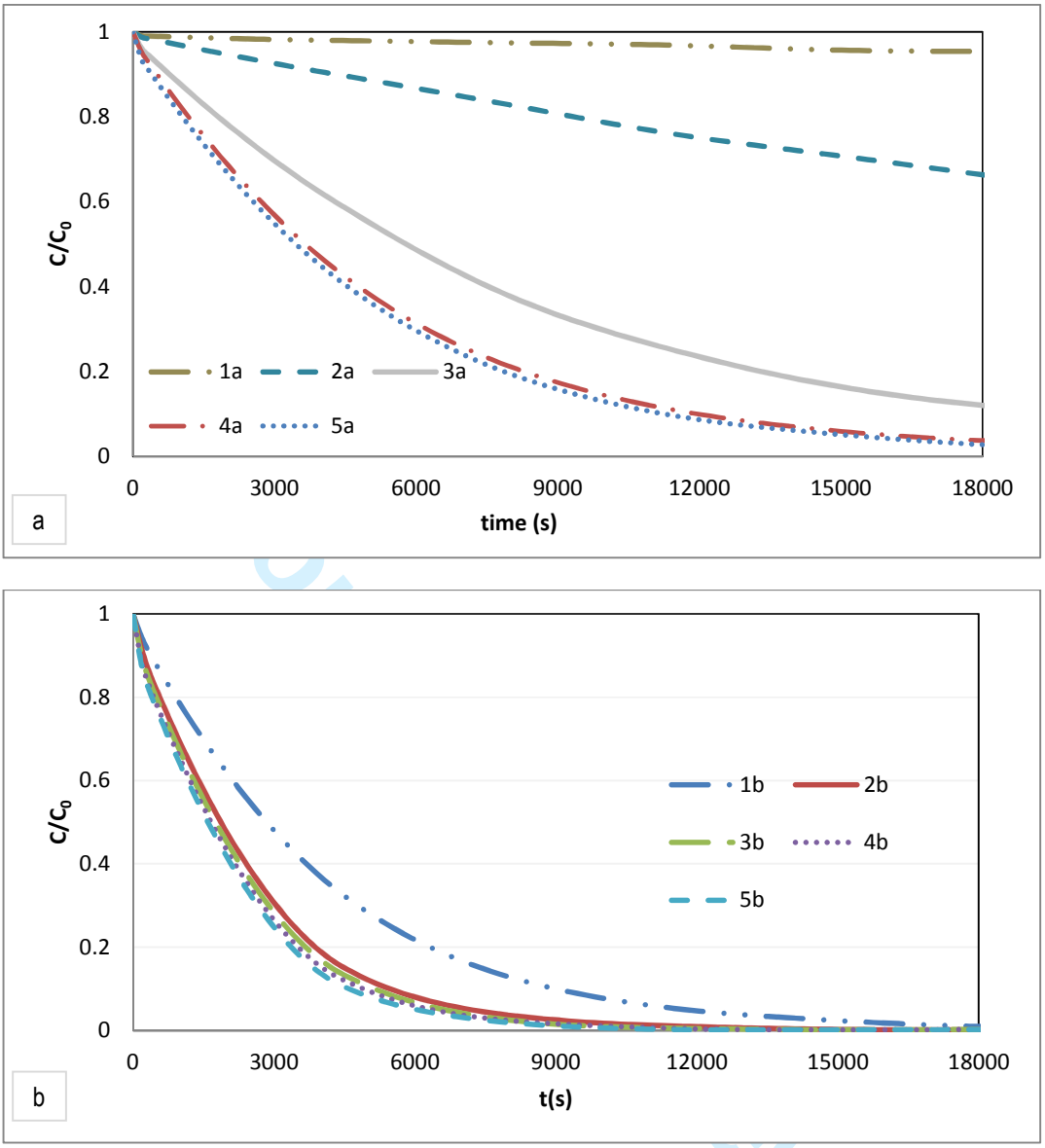

Figure 8. Evolution of the ammonia removal process for different a) pH values and b) flow rates

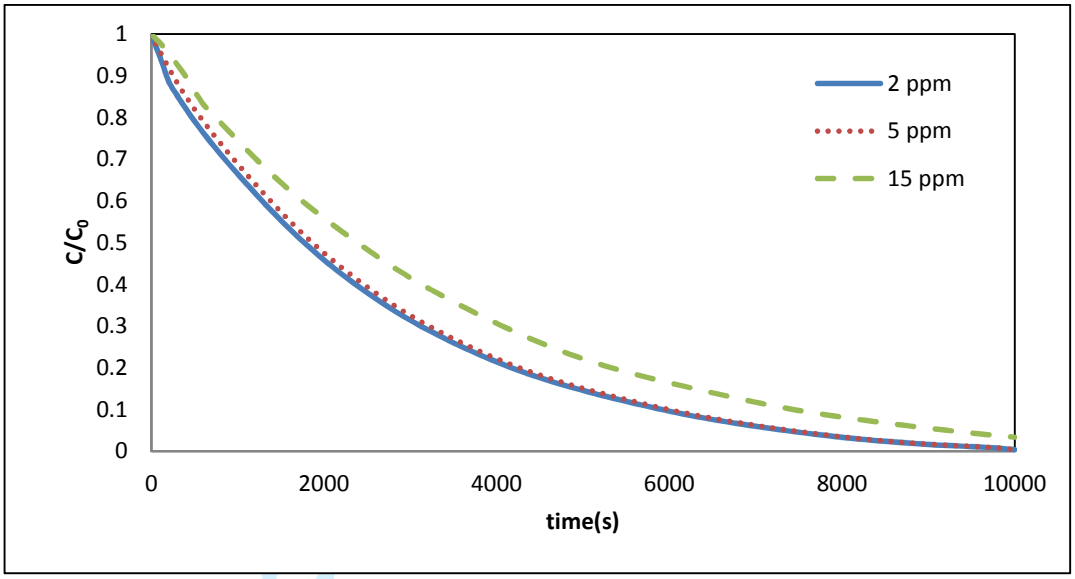

Figure 9. Concentration evolution in the feeding tank numerically simulated for different initial concentrations of ammonium C_0

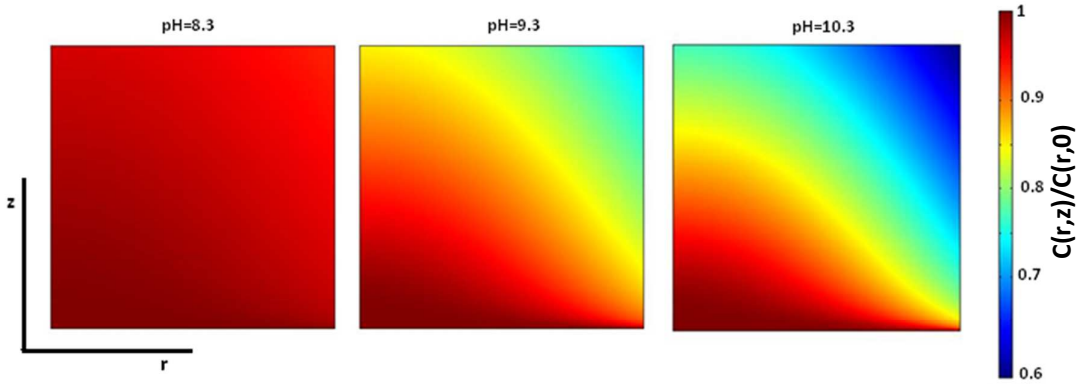

Figure 10. Ammonium concentration distribution inside the hollow fiber normalized on the value of the entrance (at z=0) for pH values of 8.3, 9.3 and 10.3

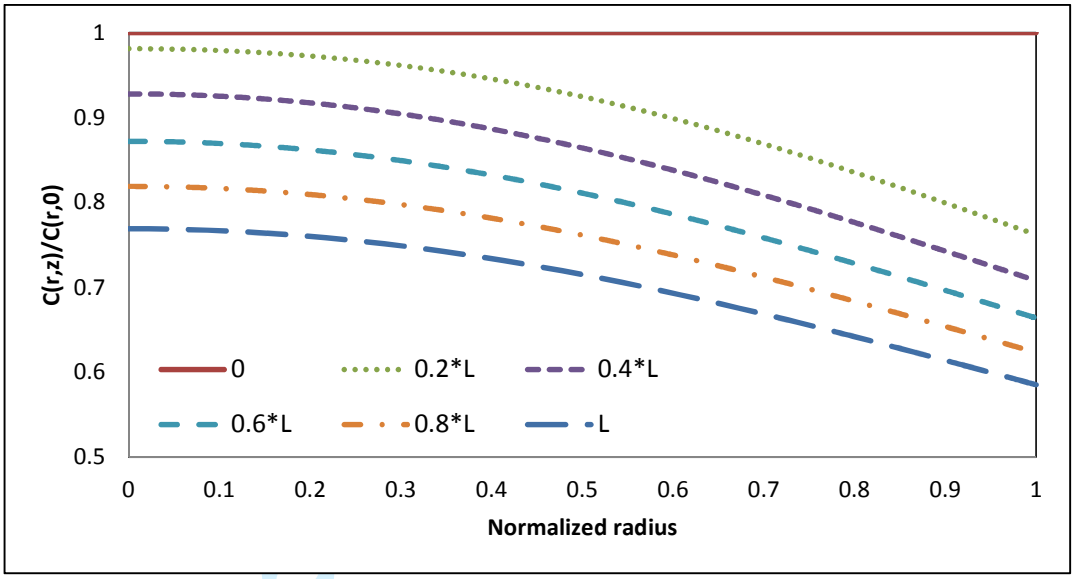

Figure 11. Radial concentration profiles of ammonium at different cross sections within the length (L) of a hollow fiber at pH=10.3